A Letters Journal Exploring the Frontiers of Physics

January 2014

EPL, **105** (2014) 18002
doi: 10.1209/0295-5075/105/18002

www.epljournal.org

Universal monomer dynamics of a two-dimensional semi-flexible chain

Aiqun Huang[1], Ramesh Adhikari[1], Aniket Bhattacharya[1] and Kurt Binder[2]

[1] *Department of Physics, University of Central Florida - Orlando, FL 32816-2385, USA*
[2] *Institut für Physik, Johannes Gutenberg-Universität Mainz - Staudinger Weg 7, 55099, Mainz, Germany*

received 1 October 2013; accepted in final form 3 January 2014
published online 31 January 2014

PACS 82.35.Lr – Physical properties of polymers
PACS 87.15.A- – Theory, modeling, and computer simulation
PACS 87.15.H- – Dynamics of biomolecules

Abstract – We present a unified scaling theory for the dynamics of monomers for dilute solutions of semi-flexible polymers under good solvent conditions in the free draining limit. Our theory encompasses the well-known regimes of mean square displacements (MSDs) of stiff chains growing like $t^{3/4}$ with time due to bending motions, and the Rouse-like regime $t^{2\nu/(1+2\nu)}$ where ν is the Flory exponent describing the radius R of a swollen flexible coil. We identify how the prefactors of these laws scale with the persistence length ℓ_p, and show that a crossover from stiff to flexible behavior occurs at a MSD of order ℓ_p^2 (at a time proportional to ℓ_p^3). A second crossover (to diffusive motion) occurs when the MSD is of order R^2. Large-scale molecular-dynamics simulations of a bead-spring model with a bond bending potential (allowing to vary ℓ_p from 1 to 200 Lennard-Jones units) provide compelling evidence for the theory, in $D = 2$ dimensions where $\nu = 3/4$. Our results should be valuable for understanding the dynamics of DNA (and other semi-flexible biopolymers) adsorbed on substrates.

Introduction and motivation. – Conformations and dynamics of semi-flexible polymers in bulk as well as under various applied fields, *e.g.*, confining and stretching potentials are of broad general interest in different disciplines of science. Important biopolymers, *e.g.*, dsDNA, F-Actin, microtubules, all have finite bending rigidity κ, often with large persistence lengths and hence the well-established and matured theories for fully flexible chains often are not adequate to describe these biopolymers as flexural rigidity plays an important role in their mechanical responses [1]. Interests in these biopolymers continue to remain unabated for multiple reasons. i) A deeper understanding of biopolymers, *e.g.*, actin, titin, fibrin which offer intriguing patterns with unusual viscoelastic responses will allow to design bio-mimetic materials with improved characteristics, not seen in synthetic polymers; ii) there is a genuine need to develop efficient separation methods of biomolecules, *e.g.*, DNA sequencing and separation of proteins for various applications pertaining to health and diseases. Finally, due to advent of sophisticated single-molecule probes, *e.g.*, fluorescence correlation spectroscopy, atomic force microscope spectroscopy, scanning electron spectroscopy with which one can directly observe the dynamics of the entire chain as well as fluorescence labeled segments of these biomolecules [2–7] which offer new findings to be further explored. Of course, also synthetic semi-flexible polymers are of interest in many circumstances; *e.g.*, adsorbed comb polymers [8] with densely packed side chains (so-called "bottle brush" polymers [9]) can be studied with atomic force microscopy [8,9] and are of interest for various applications. In these systems the persistence length can be tuned by varying the side chain length.

Historically the worm-like chain (WLC) model has been the paradigm for theoretical studies of semi-flexible chains. The Hamiltonian for the WLC is given by

$$\mathcal{H} = \frac{\kappa}{2} \int_0^L \left(\frac{\partial^2 \mathbf{r}}{\partial s^2} \right)^2 \mathrm{d}s, \tag{1}$$

where L is the contour length, κ is the bending rigidity and the integration is carried along the contour s [10,11]. One can show that in 2D and 3D dimensions $\ell_p = 2\kappa/k_BT$ and κ/k_BT, respectively [12]. The model has been studied quite extensively applying path integral and other

techniques [13–20] and exact expressions of various moments of the distribution of monomer distances along the chain have been worked out. In particular, the end-to-end distance for the WLC model is given by [10]

$$\frac{\langle R_N^2\rangle}{L^2} = \frac{2}{n_p}\left(1 - \frac{1}{n_p}[1-\exp(-n_p)]\right), \qquad (2)$$

where $L = (N-1)\delta$ is the contour length with δ being the distance between neighboring monomeric units, and $n_p = L/\ell_p$. Here we recall that any linear polymer is a chain molecule of N discrete monomeric units. In the limit $n_p \gg 1$, *i.e.*, $\ell_p \ll L$ one gets $\langle R_N^2\rangle = 2\ell_p L$ and the chain behaves like a Gaussian coil; for $n_p \ll 1$, $\langle R_N^2\rangle = L^2$ and the chain behaves like a rod. Evidently the model neglects the excluded-volume (EV) interaction and hence interpolates between rod and Gaussian limit. Dynamics of the WLC model has been explored using Langevin type of equation [17–21]. One can expect that the dynamics of a stiff-chain will be dominated by transverse fluctuations (bending modes) [16] and that the short-time dynamics will be governed by the chain persistence length. Indeed a relaxation dynamics using the WLC Hamiltonian (eq. (1)) approach yields an expression for fluctuation $\langle(\Delta h)^2\rangle \sim \ell_p^{-0.25} t^{0.75}$, which crosses over to simple diffusion at late time [17,18]. This $t^{0.75}$ behavior has been observed in many experiments using flouroscence probe and video microscopy on F-actin network [2–4] and in some simulations of polymer network [22,23]. Analytical studies of monomer dynamics in a WLC model, similar to [17,18] have been carried out for a tagged particle by Bullerjahn *et al.* [21] who also found that the transverse MSD of a tagged particle obeys subdiffusive behavior of $t^{0.75}$.

While these predictions based on WLC model are consistent with some of the experiments, the WLC model fails to capture important aspects caused by EV effects [24,25] invalidating eq. (2) in the limit $n_p \gg 1$ both in 2D and 3D where the chain statistics in D spatial dimension satisfies [26,27],

$$\sqrt{\langle R_N^2\rangle} \sim N^{\nu} \ell_p^{1/D+2} \delta^{D+1/D+2}. \qquad (3)$$

The Gaussian regime of WLC model is completely absent in 2D [24]; in 3D the Gaussian regime crosses over at $\langle R_N^2\rangle \sim \ell_p^3$ to the 3D self-avoiding walk (SAW) of eq. (3) [25]. Therefore, eq. (2) is not useful in 2D, although it is used by many authors (*e.g.*, [28]). Qualitatively, the importance of EV effects in 2D is the result of probability theory that in 2D, every random walk on a lattice eventually returns to the points already visited; Hsu *et al.* [24] have shown that eq. (2) then is accurate in the rod-like regime only. Furthermore, the angular correlation between subsequent bonds along the chain, instead of exponential, as predicted by the WLC model, exhibits a power-law decay. Therefore, EV effect has a profound effect on the statistics of stiff chains as well.

A key question is then how the EV effect affects the monomer dynamics of a semi-flexible chain. We have developed a scaling theory of monomer dynamics for a compressible semi-flexible chain. *We predict a novel double crossover dynamics where the initial subdiffusive relaxation of the monomers characterized by a $t^{0.75}$ law at an intermediate time crosses over to the monomer dynamics of a flexible chain $t^{\frac{2\nu}{1+2\nu}}$ before reaching the purely diffusive regime for the entire chain.* This is the main theoretical result of this letter. We support our claim by carrying out extensive BD simulation for a large number of chain lengths from $N = 16$ to $N = 1024$ and $\kappa = 1.0$–128, to show that i) $\langle R_N^2\rangle/(2L\ell_p)$ as a function of L/ℓ_p for all ratios L/ℓ_p collapse on the same master plot and that the early time slope of unity ($\langle R_N^2\rangle \propto L^2$; rod limit) directly crosses over to slope of 0.5 ($\langle R_N^2\rangle \propto L^{1.5}\ell_p^{0.5}$; 2D SAW, eq. (3)) clearly demonstrating the absence of Gaussian regime in 2D. ii) Second, by monitoring the dynamics of middle monomer $g_1(t) = \langle(\mathbf{r}_{N/2}(t) - \mathbf{r}_{N/2}(0))^2\rangle$, and comparing it with that of the center of mass $g_3(t) = \langle(\mathbf{r}_{CM}(t) - \mathbf{r}_{CM}(0))^2\rangle$, and the relative dynamics of $g_1(t)$ with respect to $\mathbf{r}_{CM}(t)$ expressed as $g_2(t) = \langle(\mathbf{r}_{N/2}(t) - \mathbf{r}_{CM}(t)) - (\mathbf{r}_{N/2}(0) - \mathbf{r}_{CM}(0))^2\rangle$ [29–32] we show data collapse and monomer crossover dynamics. We believe these studies of chain conformation and monomer dynamics will be extremely valuable to interpret experimental results and testing certain approximations in analytical theories for semi-flexible chains [14,19,20].

Scaling theory. – We start with the eq. (4) below derived by Granek and Maggs [17,18] using a Langevin dynamics framework for the WLC Hamiltonian of eq. (1)

$$g_1(t) = \delta^2 (\delta/\ell_p)^{1/4} (Wt)^{3/4}. \qquad (4)$$

Here we have chosen the inverse of a monomer reorientation rate W^{-1} as the unit of time. For early time the monomer dynamics will be independent of the chain length N until the fluctuations become of the order of ℓ_p. Therefore, denoting the first crossover occurs at time τ_1 and substituting $g_1 = \ell_p^2$ and $t = \tau_1$ in eq. (4) we immediately get

$$W\tau_1 = (\ell_p/\delta)^3. \qquad (5)$$

For $0 < t \leq W^{-1}(\ell_p/\delta)^3$ the monomer dynamics is described by $g_1(t) \sim t^{0.75}$ until $g_1(t) = \ell_p^2$ at time $W^{-1}(\ell_p/\delta)^3$. The width of this region is independent of N and solely a function of ℓ_p.

For $\tau_1 < t < \tau_2$ the dynamics is governed by the Rouse relaxation of monomers of a fully flexible EV chain in 2D characterized by $g_1(t) = t^{2\nu/(1+2\nu)} = t^{0.6}$. τ_2 characterizes the onset of the purely diffusive regime when $g_1(\tau_2) = \langle R_N^2\rangle$ [29]. We then obtain τ_2 as follows:

$$g_1(t) = \ell_p^2 (t/\tau_1)^{3/5}, \quad \text{for } t > \tau_1. \qquad (6)$$

Substituting τ_1 from eq. (5) in the above

$$g_1(t) = \delta^2 (\ell_p/\delta)^{1/5} (Wt)^{3/5}, \quad \text{for } \tau_1 < t < \tau_2. \qquad (7)$$

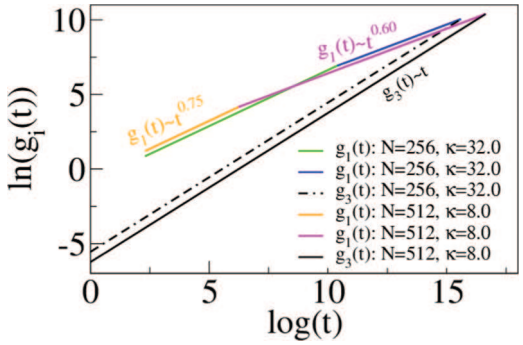

Fig. 1: (Colour on-line) Theoretical scaling plots for $(N, \kappa) \equiv (256, 32)$ and $(N, \kappa) \equiv (512, 8)$. Green and orange lines correspond to $g_1(t) \sim t^{0.75}$, blue and magenta lines correspond to $g_1 \sim t^{0.60}$, and the dashed and solid black lines correspond to $g_3(t) \sim t$ for $N = 256$ and 512, respectively. The width of each region shows how these regimes depend on ℓ_p and N. Note that in reality we expect a very gradual change of slope on the log-log plot at both crossover times, rather than sharp kinks.

At $t = \tau_2$

$$g_1(t = \tau_2) = \langle R_N^2 \rangle = \ell_p^{1/2} \delta^{3/2} N^{3/2}. \tag{8}$$

Substituting eq. (7) for $t = \tau_2$ we get

$$W\tau_2 = (\ell_p/\delta)^{\frac{1}{2}}\, N^{5/2}. \tag{9}$$

We also note that the dynamics of the center of mass is given by (omitting prefactors of order unity throughout)

$$g_3(t) = \delta^2 W \frac{t}{N}. \tag{10}$$

The "phase diagram" for the crossover dynamics in terms of N, and ℓ_p is shown in fig. 1. Notice that for a stiffer chain the region for $\tau_1 < t < \tau_2$, for which we predict $g_1(t) \sim t^{0.6}$, becomes progressively small and therefore, is hard to see in simulation for a stiffer chain.

Model and simulation results. – For polymers confined on a 2D surface the hydrodynamic interactions are essentially screened [33]. Hence we have used an ordinary BD scheme to advance the position of the i-th monomer $\vec{r}_i$ with the following equation of motion:

$$m\ddot{\vec{r}}_i = -\nabla(U_{\rm LJ} + U_{\rm FENE} + U_{\rm bend}) - \Gamma\vec{v}_i + \vec{\eta}_i. \tag{11}$$

Here $U_{\rm LJ}(r) = 4\epsilon[(\frac{\sigma}{r})^{12} - (\frac{\sigma}{r})^{6}] + \epsilon$ for $r \le 2^{1/6}\sigma$, and zero otherwise, σ is the effective diameter of a monomer, and ϵ is the strength of the potential; the chain connectivity is described by $U_{\rm FENE}(r) = -\frac{1}{2}kR_0^2 \ln(1 - r_{ij}^2/R_0^2)$, where $\vec{r}_{ij} = \vec{r}_i - \vec{r}_j$, k is the spring constant and R_0 is the maximum allowed separation between connected monomers [29], and $U_{\rm bend}(\theta_i) = \kappa(1 - \cos\theta_i)$ represent the three-body bond bending potential, where θ_i is the angle between the bond vectors $\vec{b}_{i-1} = \vec{r}_i - \vec{r}_{i-1}$ and $\vec{b}_i = \vec{r}_{i+1} - \vec{r}_i$, respectively, and κ is the measure of the strength of the interaction. Γ is the monomer friction coefficient and $\vec{\eta}_i(t)$ is a Gaussian white noise with zero mean at a temperature T, and satisfies the fluctuation-dissipation relation: $\langle \vec{\eta}_i(t) \cdot \vec{\eta}_j(t') \rangle = 4k_BT\Gamma\, \delta_{ij}\, \delta(t - t')$ in 2D. The reduced units of length, time, and temperature are chosen to be σ, $\sigma\sqrt{\frac{m}{\epsilon}}$, and ϵ/k_B, respectively. For the spring potential we have chosen $k = 30$ and $R_0 = 1.5\sigma$, the friction coefficient $\Gamma = 0.7$, the temperature is kept at $1.2/k_B$.

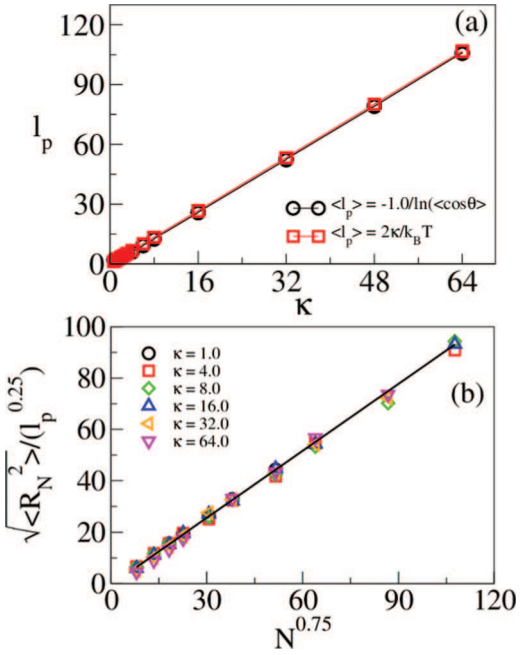

Fig. 2: (Colour on-line) (a) Comparison of $\ell_p = -1/\ln(\langle\cos\theta\rangle)$ and $\ell_p = 2\kappa/k_BT$. (b) Plot of $\sqrt{\langle R_N^2\rangle}/\ell_p^{0.25}$ *vs.* $N^{0.75}$ for various values of the chain stiffness parameter. All the data for different stiffness parameters collapse on the same master plot. The solid line is a fit to a straight line.

We first calculated the chain persistence length ℓ_p as a function of the bending rigidity κ. It is worth noting that the persistence length must not be extracted from the decay of bond orientational correlations at large distances along the chain, but even in the presence of the EV interaction it still can be estimated from the average $\langle\cos\theta\rangle$ between subsequent bonds by the standard formula $\ell_p = -1/\ln\langle\cos\theta\rangle$. We find that this estimate also coincides with the continuum theory result $\ell_p = 2\kappa/k_BT$ [10] as shown in fig. 2(a) where we have used $\langle\cos\theta\rangle$ obtained from the simulation to calculate ℓ_p for different combination of κ and N. Since the persistence length is an intrinsic local property of the chain, EV has very little effect on it. This, although not the main focus of this letter, is a new result[1]. Using ℓ_p obtained from simulation we then

[1]It is worth mentioning that a very common used definition of persistence length in the literature is $\langle \vec{b}_1 \cdot \vec{R}_N \rangle$ [13,34] and has been used in simulations [35]. An end-to-end vector cannot be a good candidate to explore the local property of a chain, especially for long chains [36]. We have checked that this definition does not simply work and is somewhat misleading.

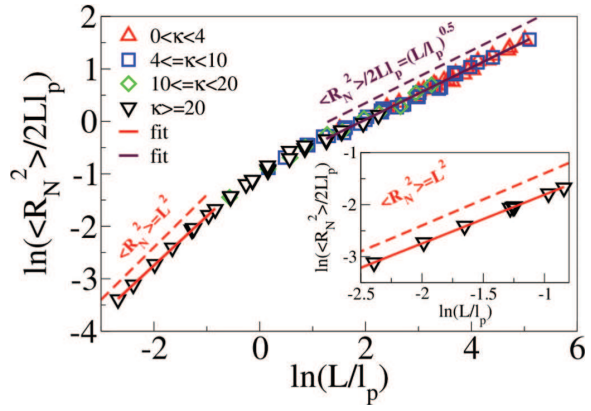

Fig. 3: (Colour on-line) $\langle\langle R_N^2\rangle/(2L\ell_p)$ as a function of L/ℓ_p obtained from different combinations of the chain length N and the stiffness parameter κ (log-log scale). The solid (maroon) line is a fit to the formula $\langle R_N^2\rangle/2L\ell_p \sim (L/\ell_p)^{0.5}$ for $4 < L/\ell_p < 160$. The inset shows the same for small values of $0 < L/\ell_p < 1$ which clearly indicates that limiting slope of unity ($\langle R_N^2\rangle = L^2$) for $L/\ell_p \to 0$.

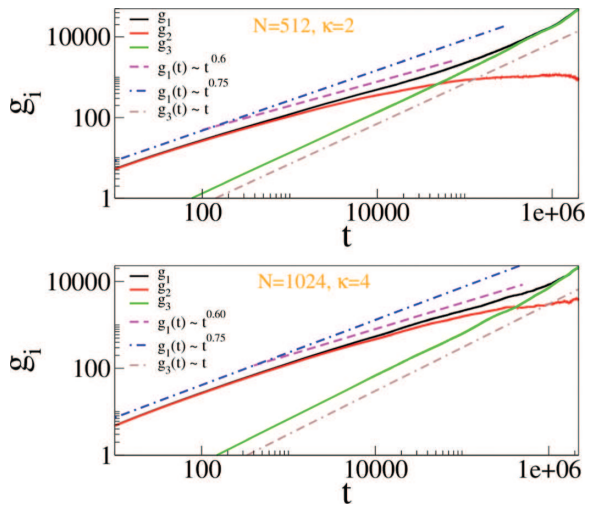

Fig. 4: (Colour on-line) Top: plot for $g_1(t)$ (black), $g_2(t)$ (red) and $g_3(t)$ (green) as a function of time on a log-log scale for chain length $N = 512$ and $\kappa = 2.0$. The blue and magenta dashed lines correspond to straight lines $g_1(t) = At^{0.75}$, and $g_1(t) = Bt^{0.60}$, respectively, where A and B are constants. Bottom: same but for $N = 1024$ and $\kappa = 4.0$. Note that for a fully flexible chain the slope of the curve $\log(g_i)$ *vs.* $\log(t)$ would monotonously increase with time, unlike in the present case.

verified that in 2D the end-to-end distance satisfies the relation $\sqrt{\langle R_N^2\rangle} \sim N^\nu \ell_p^{0.25}$ [26,27] for various combinations of ℓ_p and chain length N [37] as shown in fig. 2(b).

Figure 3 shows a plot of $\langle R_N^2\rangle/2\ell_p L$ as a function of L/ℓ_p for a huge number of values of L/ℓ_p (~ 100).

For $L/\ell_p \ll 1$ we observe that $\frac{\langle R_N^2\rangle}{2\ell_p L} \sim (L/\ell_p)^{1.0}$, while for $L/\ell_p \gg 1$ the data very nicely fit with $\frac{\langle R_N^2\rangle}{2\ell_p L} \sim (L/\ell_p)^{0.50}$. This plot for chains with varying degree of stiffness and chain length conclusively shows the absence

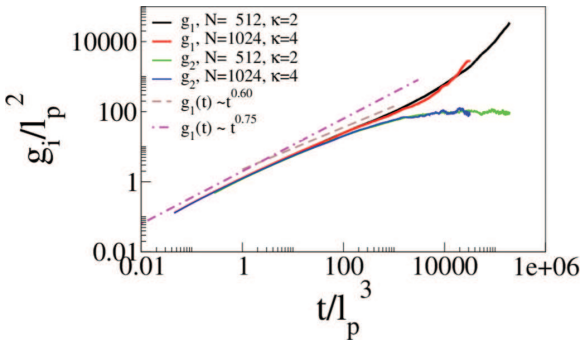

Fig. 5: (Colour on-line) Plot for $g_1(t)/\ell_p^2$ (black and red) and $g_2(t)/\ell_p^2$ (blue and green) as a function of t/ℓ_p^3 on a log-log scale for chain lengths $N = 512$, $\kappa = 2.0$ and for $N = 1024$, $\kappa = 4.0$ respectively. The dot-dashed lines correspond to slopes 0.75 (magenta) and 0.6 (brown) respectively.

of Gaussian regime in a 2D EV chain earlier observed by Hsu *et al.* from a lattice model [24] and observed in experiments with single-stranded DNA on modified graphite substrate [7].

We now present BD simulation results to confirm our scaling theory. Results for $g_1(t)$, $g_2(t)$, and $g_3(t)$ shown in fig. 4 unambiguously confirm our predictions. These plots quite clearly show three distinct scaling regimes of $g_1(t) \sim t^{0.75}$ crossing over to $g_1(t) \sim t^{0.6}$ and then merging with $g_3(t) \sim t$ at late times. The double crossover required simulation of reasonably large chain lengths ($N = 512 - 1024$) below which it is hard to see these crossovers conclusively[2]. Figure 5 shows plot of $g_1(t)/\ell_p^2$ as a function of rescaled time t/ℓ_p^3 which shows data collapse for various chain lengths N and κ again confirming the time scales for these crossovers. As expected, the crossovers are rather gradual, spread out over a decade in time t each, and hence for chains that are not long enough the existence of these regimes is missed in less careful work.

Discussion and conclusions. – To summarize, we have provided a new scaling theory of monomer dynamics for semi-flexible polymers in 2D. Our theory predicts novel crossover dynamics at an intermediate time when the fluctuations of the monomers become greater than ℓ_p. Around this time the monomer dynamics becomes the same as that of a fully flexible chain characterized by $g_1(t) \sim t^{2\nu/(1+2\nu)} = t^{0.6}$ in 2D. The theory expands the existing scaling theory for monomer dynamics for a WLC and that of a fully flexible chain to include the effect of the chain persistence length. Fully flexible chains are self-similar objects, while a polymer segment up to its own persistence length is not. Therefore, it is expected that for a length scale up to ℓ_p the dynamics will have different characteristics due to bending modes arising out of the chain stiffness. The EV effect is almost negligible for the

[2]The internal dynamics is strictly visible in the quantity $g_2(t)$, which unlike $g_1(t)$, does not show a $t^{0.6}$ behavior over a similar time scale. This we believe is due to finite-size effects. We thank one of the referees for pointing it out.

$t^{0.75}$ regime and therefore, our result is the same as that of previous studies using the WLC Hamiltonian [17,18]. For the $t^{0.6}$ regime originating from the EV effect, where the monomer dynamics is governed by the Rouse relaxation of a fully flexible chain, our theory elucidates the exact role of chain persistence length neither contained in the WLC model nor seen before. We also validate our new scaling theory by extensive BD simulation results.

We now comment on the generalization of our results in 3D and/or in the presence of hydrodynamic (HD) interactions. In the free draining limit the $t^{0.75}$ regime will remain the same in 3D [17,18], but the intermediate Rouse relaxation regime will be characterized by $t^{2\nu/(1+2\nu)} = t^{0.54}$ ($\nu = 0.59$ in 3D). Replacing Rouse relaxation by Zimm relaxation one immediately sees that in the presence of HD interaction the intermediate regime is characterized by $\sim t^{2\nu/3\nu} = t^{2/3}$ [38–40]. Notice that in this case ν cancels out and this relaxation should be the same in 2D and 3D. The exponent 2/3 has been seen experimentally in segmental dynamics of fluorescent labeled λ-phage DNA by Petrov *et al.* [6] and analyzed theoretically by Hinczewski and Netz [39,40].

Finally, we provide a plausible explanation why this double crossover is hard to see in single-molecule experiments with biopolymers [2–6]. First of all, lacking any theoretical predictions for this phenomenon, researchers did not specifically investigate the precise behavior of MSD before the onset of overall chain diffusion very carefully. A direct analysis of the MSD of an end labeled polymer requires extreme caution for a time much shorter than the longest relaxation time [6]. Much care indeed is needed, as the following argument shows: a simple calculation for fig. 1 shows that in order for the width of the $t^{0.75}$ and $t^{0.60}$ to be equal (in logarithmic scale) one needs $N = l_p^{2.2}$ in 2D. In other words for a stiffer chain one needs a very long chain to see the $t^{0.60}$ regime. Indeed in our simulation we found (not shown here) that for $\kappa = 16$, 32, and 64, the results with a chain length up to $N = 512$ are largely dominated by the $t^{0.75}$ regime and we did not clearly see the $t^{0.60}$ regime. It is only after we lowered the value of κ and used a longer chain ($N = 1024$), we identified these two regimes quite conclusively (fig. 4). We suspect that the same might happen in experiments [2]. For extreme stiff chains the $t^{0.6}$ (or $t^{0.54}$ in 3D) region can be extremely narrow and could either be missed or the rather smooth double crossover might be mistakenly interpreted as a single crossover (with $t^{2/3}$ in 2D). Therefore, we believe that these results will not only promote new experiments but will be extremely valuable in identifying and interpreting different scaling regimes for the monomer dynamics of semi-flexible polymers.

* * *

AB, AH, and RA acknowledge financial support through a seed grant from UCF. AB acknowledges travel support from Prof. K. Binder. We thank all the reviewers for their constructive criticism and comments on the manuscript.

REFERENCES

[1] Phillips R., Kondev J. and Theriot J., *Physical Biology of the Cell* (Garl and Science) 2009.
[2] Dichtl M. A. and Sackmann E., *New J. Phys.*, **1** (1999) 18.
[3] Le Goff L., Hallatschek O., Frey E. and Amblard F., *Phys. Rev. Lett.*, **89** (2002) 25801.
[4] Caspi A., Elbaum M., Granek R., Lachish A. and Zbaida D., *Phys. Rev. Lett.*, **80** (1998) 1106.
[5] Shusterman R., Alon S., Gavrinyov T. and Krichevsky O., *Phys. Rev. Lett.*, **92** (2004) 048303.
[6] Petrov E. P., Ohrt T., Winkler R. G. and Schwille P., *Phys. Rev. Lett.*, **97** (2006) 258101.
[7] Rechendorff K., Witz G., Adamik J. and Dietler G., *J. Chem. Phys.*, **131** (2009) 095103.
[8] Sheiko S., Sumerlin B. S. and Matyjaszewski K., *Prog. Polym. Sci.*, **33** (2008) 759.
[9] Gunari N., Schmidt M. and Janshoff A., *Macromolecules*, **39** (2006) 2219.
[10] Rubinstein M. and Colby R. H., *Polymer Physics* (Oxford University Press) 2003.
[11] Doi M. and Edwards S. F., *Theory of Polymer Dynamics* (Clarendon Press, Oxford) 1986.
[12] Landau L. D. and Lifshitz E. M., *Statistical Physics, Part 1*, 3rd edition (Pergamon Press) 1988.
[13] Yamakawa H., *Modern Theory of Polymer Solution*, (Harper & Row Publishers) 1971.
[14] Harnau L., Winkler R. G. and Reineker P., *EPL*, **45** (1999) 488.
[15] Harnau L., Winkler R. G. and Reineker P., *J. Chem. Phys.*, **104** (1996) 6355.
[16] Winkler R. G., *J. Chem. Phys.*, **118** (2003) 2919.
[17] Granek R., *J. Phys. II*, **7** (1997) 1767.
[18] Farge E. and Maggs A. C., *Macromolecules*, **26** (1993) 5041.
[19] Kroy K. and Frey E., *Phys. Rev. E*, **55** (1997) 3091.
[20] Wilhelm J. and Frey E., *Phys. Rev. Lett.*, **77** (1996) 2581.
[21] Bullerjahn J. T., Sturm S., Wolff L. and Kroy K., *EPL*, **96** (2011) 48005.
[22] Bulacu M. and van der Giessen E., *J. Chem. Phys.*, **123** (2005) 114901.
[23] Steinhauser M. O., Schneider J. and Blumen A., *J. Chem Phys.*, **130** (2009) 164902.
[24] Hsu H.-P., Paul W. and Binder K., *EPL*, **95** (2011) 68004.
[25] Hsu H.-P., Paul W. and Binder K., *EPL*, **92** (2010) 28003.
[26] Schaefer D. W., Joanny J. F. and Pincus P., *Macromolecules*, **13** (1980) 1280.
[27] Nakanishi H., *J. Phys. (Paris)*, **48** (1987) 979.
[28] Moukhtar J., Fontaine E., Faivre-Moskalenko C. and Arneodo A., *Phys. Rev. Lett.*, **98** (2007) 178101.
[29] Grest G. S. and Kremer K., *Phys. Rev. A*, **33** (1986) 3628.
[30] Gerroff I., Milchev A., Paul W. and Binder K., *J. Chem. Phys.*, **33** (1992) 6526.

[31] Milchev A., Paul W. and Binder K., *J. Chem. Phys.*, **99** (1993) 4786.
[32] Binder K. and Paul W., *J. Polym. Sci. B*, **35** (1997) 1.
[33] Winkler A., Virnau P., Binder K., Winkler R. G. and Gompper G., *J. Chem. Phys.*, **138** (2013) 054901.
[34] Redner S. and Privman V., *J. Phys. A: Math. Gen.*, **20** (1987) L857.
[35] Cifra P., *Polymer*, **45** (2004) 5995.
[36] Hsu H.-P., Paul W. and Binder K., *Macromolecules*, **43** (2010) 3094.
[37] Adhikari R. and Bhattacharya A., *J. Chem. Phys.*, **138** (2013) 240909.
[38] Hinczewski M., Schlagberger X., Rubinstein M., Krichevsky O. and Netz R. R., *Macromolecules*, **42** (2009) 860.
[39] Hinczewski M. and Netz R. R., *EPL*, **88** (2009) 18001.
[40] Hinczewski M. and Netz R. R., *Physica A*, **389** (2010) 2993.